ARMY RESEARCH LABORATORY

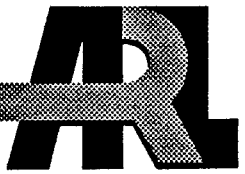

Analytical Potential Energy Surface for Methylene Nitramine (CH_2NNO_2)

Betsy M. Rice
George F. Adams
U.S. ARMY RESEARCH LABORATORY

Michael Page
NORTH DAKOTA STATE UNIVERSITY

Donald L. Thompson
OKLAHOMA STATE UNIVERSITY

ARL-TR-680 February 1995

NOTICES

Destroy this report when it is no longer needed. DO NOT return it to the originator.

Additional copies of this report may be obtained from the National Technical Information Service, U.S. Department of Commerce, 5285 Port Royal Road, Springfield, VA 22161.

The findings of this report are not to be construed as an official Department of the Army position, unless so designated by other authorized documents.

The use of trade names or manufacturers' names in this report does not constitute endorsement of any commercial product.

REPORT DOCUMENTATION PAGE

Form Approved
OMB No. 0704-0188

1. AGENCY USE ONLY (Leave blank)	2. REPORT DATE	3. REPORT TYPE AND DATES COVERED
	February 1995	Final, Sep 93–Jun 94

4. TITLE AND SUBTITLE

Analytical Potential Energy Surface for Methylene Nitramine (CH_2NNO_2)

5. FUNDING NUMBERS

PR: 1L161102AH43

6. AUTHOR(S)

Betsy M. Rice, George F. Adams, Michael Page,* and Donald L. Thompson**

7. PERFORMING ORGANIZATION NAME(S) AND ADDRESS(ES)

U.S. Army Research Laboratory
ATTN: AMSRL-WT-PC
Aberdeen Proving Ground, MD 21005-5066

8. PERFORMING ORGANIZATION REPORT NUMBER

9. SPONSORING / MONITORING AGENCY NAME(S) AND ADDRESS(ES)

U.S. Army Research Laboratory
ATTN: AMSRL-OP-AP-L
Aberdeen Proving Ground, MD 21005-5066

10. SPONSORING / MONITORING AGENCY REPORT NUMBER

ARL-TR-680

11. SUPPLEMENTARY NOTES

* Professor Page is employed by North Dakota State University.
** Professor Thompson is employed by Oklahoma State University.

12a. DISTRIBUTION / AVAILABILITY STATEMENT

Approved for public release; distribution is unlimited.

12b. DISTRIBUTION CODE

13. ABSTRACT *(Maximum 200 words)*

An analytic potential energy surface (PES) that accurately describes the reaction of CH_2NNO_2 was developed. The surface is based on MCSCF and MRCI calculations of Mowrey et al. (1990). The two primary decomposition pathways that can be described by this PES are (I) N–N bond scission to form H_2CN and NO_2 and (II) concerted dissociation via a five-center transition state to eliminate HONO + HCN. The classical barrier heights differ by 2 kcal/mol. Thermal rates, calculated with Variational Transition State Theory, were used to parameterize this function to agree with the Mowrey et al. results. This model can be used in molecular dynamics or Monte Carlo simulations for this chemical system.

14. SUBJECT TERMS	15. NUMBER OF PAGES
potential energy surface, methylene nitramine molecular dynamics, unimolecular decomposition	27
	16. PRICE CODE

17. SECURITY CLASSIFICATION OF REPORT	18. SECURITY CLASSIFICATION OF THIS PAGE	19. SECURITY CLASSIFICATION OF ABSTRACT	20. LIMITATION OF ABSTRACT
UNCLASSIFIED	UNCLASSIFIED	UNCLASSIFIED	UL

INTENTIONALLY LEFT BLANK.

ACKNOWLEDGMENTS

The authors wish to thank Dr. Gillian Lynch for helpful discussions regarding Variational Transition State Theory and use of POLYRATE 5.0.1. Donald L. Thompson gratefully acknowledges support from the U.S. Army Research Office. Michael Page acknowledges support from the Mechanics Division of the Office of Naval Research through Grant No. N000149310045. Some of the calculations were performed at the Department of Defense (DOD) High-Performance Computing Center (HPC) at the Corps of Engineers Waterways Experimental Station (CEWES), Vicksburg, MS.

INTENTIONALLY LEFT BLANK.

TABLE OF CONTENTS

INTENTIONALLY LEFT BLANK.

LIST OF FIGURES

INTENTIONALLY LEFT BLANK.

LIST OF TABLES

INTENTIONALLY LEFT BLANK.

1. INTRODUCTION

CH_2NNO_2, or methylene nitramine (MN), is thought to be one of the primary decomposition products of hexahydro-1,3,5-trinitro-1,3,5-triazine (RDX) (Schroeder 1985a, 1985b). MN has never been isolated and is believed to decompose spontaneously after formation through concerted channels only (Zhao, Hintsa, and Lee 1988). Scission of the weakest bond in MN (the N–N bond) is not observed (Zhao, Hintsa, and Lee 1988), which is a surprising result. One explanation could be simply that energy required for reaction through concerted channels is substantially lower than the scission reaction. Another explanation is that there is anomalous dynamical behavior in the system. We wish to perform molecular dynamics simulations of the decomposition of MN, but to do so requires an analytic potential energy surface (PES) that accurately describes the system and reaction channels. The development of such a PES is the focus of this report.

The only characterizations of MN come from theoretical predictions. Thus, we are limited in the information that we can use to construct a potential energy function of this molecule. We based the PES of MN that we developed in this work on the ab initio multiconfigurational (MC) SCF and multireference (MR) CI electronic structure calculations of Mowrey et al. (Mowrey et al. 1990; Mowrey unpublished). In that work, they examined what they believed to be the primary decomposition channels for MN:

$$CH_2NNO \rightarrow H_2CN + NO_2 \qquad \text{(I)}$$

and

$$CH_2NNO_2 \rightarrow HCN + HONO. \qquad \text{(II)}$$

They calculated the structure, relative energies, and frequencies of equilibrium MN, the five-centered transition state for HONO elimination, and the products for the two reactions (Mowrey et al. 1990). Additionally, they calculated points along the reaction path from the five-centered transition state of (II) leading to reactants (MN) and products (HONO + HCN) (Mowrey et al. unpublished). The structures of the planar equilibrium MN and five-centered transition state leading to HONO + HCN are shown in Figure 1. After adjusting for zero-point energy effects, basis sets and different levels of theory, they estimate that the activation energy for (II) is 31 ± 4 kcal/mol. They also estimate the N–N bond dissociation energy for (I) to be 35 ± 4 kcal/mol. Although these estimates suggest that reaction (II) is

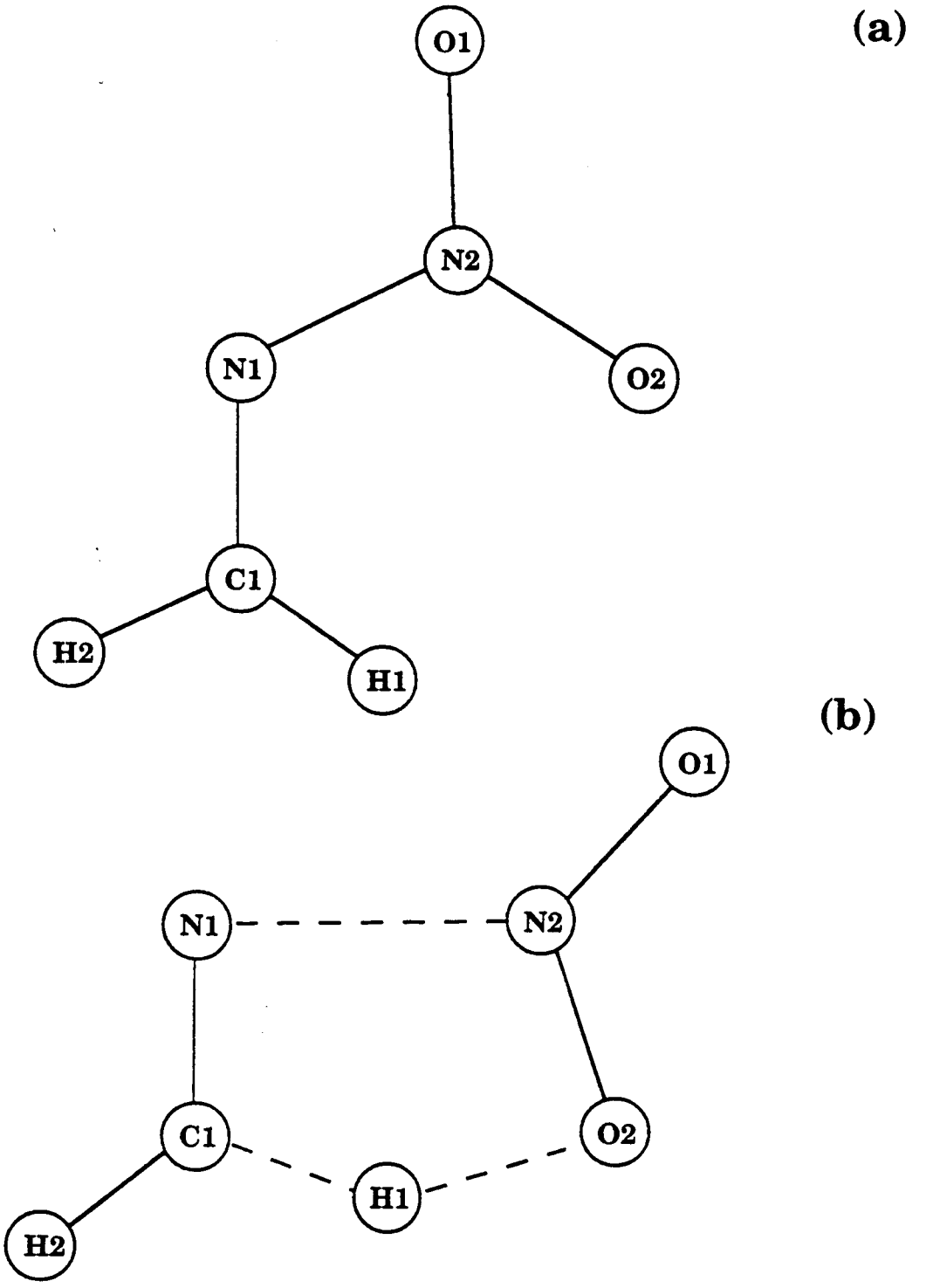

Figure 1. Structures obtained at the 8-in-8 CASSCF/DZP level (see Mowrey et al. 1990) for a) equilibrium MN and b) the five-centered transition state leading to HONO + HCN.

energetically favored, the steric effects associated with reaction (II) would make reaction (I) entropically favored.

Mowrey et al. (1990) have shown that the activation energy for (II) is lower than, or at least comparable with, the N–N bond dissociation energy. The analytic PES that we report here, based on the Mowrey et al. calculations (Mowrey et al. 1990; unpublished), can be used in molecular dynamics simulations to investigate whether MN exhibits dynamical behavior that would preclude reaction (I).

2. POTENTIAL ENERGY SURFACE (PES)

2.1 Analytical Form of the Potential. The total potential energy expression is:

$$
\begin{aligned}
V = {} & V^{s}_{OH} + V^{s}_{CN} + V^{s}_{NN} + \sum_{i=1}^{2} V^{s}_{CH(i)} + \sum_{i=1}^{2} V^{s}_{NO(i)} + V^{b}_{HCH} + \sum_{i=1}^{2} V^{b}_{NCH(i)} \\
& + \left(V^{b}_{CNN} + \sum_{i=1}^{2} V^{b}_{NNO(i)} + \sum_{i=1}^{2} V^{\tau}_{CNNO(i)} + \sum_{i=1}^{2} V^{\tau}_{NNCH(i)} + V^{\omega}_{NNO_2} \right) \cdot S_{TT} \\
& + \left(V^{b}_{ONO} + V^{b}_{HON} \right) \cdot S_{HONO} + V^{\omega}_{H_2CN} \cdot S_{Pro} \\
& + \left\{ \sum_{i=14}^{17} \left[V^{i}_{HONO} \cdot S_i \right] \right\} \cdot S_{HONO} \cdot \left(1 - S_{Pro} \right),
\end{aligned}
\tag{1}
$$

where V^{s} is the Morse function that describes bond stretches, V^{b} is a harmonic oscillator function that describes bending motions, and V^{ω}, V^{τ}, and V_{HONO} are functions of cosines describing out-of-plane wagging and torsional motions.

These simple functions (V^{2}, V^{b}, V^{ω}, and V^{τ}, defined in subheadings in Table 1) are not flexible enough to describe correctly the system at all regions of the PES if constant parameters are used. Many of the parameters for these functions must have significantly different values at the product geometry than at the reactant geometry. For example, the C–N bond in the product HCN is much stronger than the C–N bond in the reactant CH_2NNO_2. Therefore, constant parameters for the C–N interaction terms would not

Table 1. Potential Energy Functions and Parameters

$V^S = D\{1 - \exp(-\alpha[r - r_e])\}^2 - D$

CN

Parameter	Type	X	A	B	C	R_0
D	P(−)	R_{OH-NN}	0.847500	3.232720	5.900000	−0.666680
α	P(+)	R_{OH-NN}	−0.151844	0.773610	2.710000	0.000000
r_e	P(+)	R_{OH-NN}	0.060691	2.497460	1.149500	−0.760780

NN

Parameter	Type	X	A	B	C	R_0
D	P(+)	R_{OH-NN}	0.759000	4.136200	0.000000	−1.321150
α	P(+)	R_{OH-NN}	1.229500	0.975370	0.000000	−0.164100
r_e	P(−)	R_{OH-NN}	1.062930	2.529080	1.441141	−0.787890

CH $\quad Y_{[CH(1)]} = Y_A(S_{14} + S_{15}) + Y_B(S_{16} + S_{17})$, $\quad Y_{[CH(2)]} = Y_B(S_{14} + S_{15}) + Y_A(S_{16} + S_{17})$ $\quad$ Y = D, α, or r_e

Parameter	Type	X	A	B	C	R_0
D_A	P(+)	R_{OH-NN}	2.168000	2.760820	0.000000	−0.652960
α_A	P(+)	R_{OH-NN}	1.069000	1.942640	0.000000	−0.952120
$r_{e\,A}$	Constant		1.073393			
D_B	P(−)	R_{OH-NN}	0.365500	1.965080	4.336000	−0.970880
α_B	P(+)	R_{OH-NN}	0.128000	0.263500	1.895000	0.000000
r_{eB}	P(+)	R_{OH-NN}	0.002680	2.685560	1.065370	−1.042670

NO $\quad D = D^{Product} + (D^{Reactant} - D^{Product})\, S_{HONO}$ $\quad Y_{[NO(1)]} = Y_A(S_{14} + S_{16}) + Y_B(S_{15} + S_{17})$, $\quad Y_{[NO(2)]} = Y_B(S_{14} + S_{16}) + Y_A(S_{15} + S_{17})$ $\quad Y = D^{Reactant}$, α, or r_e

Parameter	Type	X	A	B	C	R_0
$D^{Product}$	Constant		6.614000			
D_A	P(+)	R_{OH-NN}	0.488000	2.766320	3.451000	−1.229720
α_A	P(+)	R_{OH-NN}	0.505000	2.500000	1.350000	0.000000
$r_{e\,A}$	P(−)	R_{OH-NN}	0.048115	2.591180	1.303440	−0.625800
D_B	P(−)	R_{OH-NN}	0.675500	3.101050	4.427000	−0.761420
α_B	P(−)	R_{OH-NN}	0.101000	2.500000	2.360000	0.000000
r_{eB}	P(+)	R_{OH-NN}	0.037044	2.648640	1.166310	−0.978410

HO $\quad Y = Y^{Product} + (Y^{Reactant} - Y^{Product})\, S_{HONO}$, $\quad Y = D^{Reactant}$, $\alpha^{Reactant}$

Parameter	Type	X	A	B	C	R_0
$D^{Product}$	Constant		4.624000			
$\alpha^{Product}$	Constant		2.293640			
$D^{Reactant}$	P(−)	R_{OH-NN}	2.132500	2.604230	0.000000	−1.252450
$\alpha^{Reactant}$	P(+)	R_{OH-NN}	2.179910	3.127710	2.296000	0.000000
r_e	Constant		0.954106			

Table 1. Potential Energy Functions and Parameters (continued)

$V^B = k\,(\Theta - \Theta_e)^2$

HCH

Parameter	Type	X	A	B	C	R_0
k	P(+)	R_{OH-NN}	0.641699	2.851970	0.000000	−0.000020
Θ_e	Constant		119.91592			

CNN

Parameter	Type	X	A	B	C	R_0
k	P(+)	R_{OH-NN}	1.712481	2.797200	0.000000	−0.839420
Θ_e	Constant		115.72031			

ONO

Parameter	Type	X	A	B	C	R_0
k	P(−)	R_{OH-NN}	1.337147	4.363370	3.530805	0.000000
Θ_e	P(+)	R_{OH-NN}	6.539728	3.084920	111.38000	−0.752150

HCN $Y_{[NCH(1)]} = Y_A(S_{14} + S_{15}) + Y_B(S_{16} + S_{17})$, $Y_{[NCH(2)]} = Y_B(S_{14} + S_{15}) + Y_A(S_{16} + S_{17})$ Y = k or Θ_e

Parameter	Type	X	A	B	C	R_0
k_A	P(+)	R_{OH-NN}	1.198696	3.313430	0.000000	−0.743490
$\Theta_{e\,A}$	Constant		124.12487			
k_B	P(+)	R_{OH-NN}	0.799410	3.882660	0.000000	−0.373060
$\Theta_{e\,B}$	P(−)	R_{OH-NN}	32.020394	2.128550	115.95921	−1.029180

NNO $Y_{[NNO(1)]} = Y_A(S_{14} + S_{16}) + Y_B(S_{15} + S_{17})$, $Y_{[NNO(2)]} = Y_B(S_{14} + S_{16}) + Y_A(S_{15} + S_{17})$ Y = k or Θ_e

Parameter	Type	X	A	B	C	R_0
k_A	P(+)	R_{OH-NN}	1.814668	1.765720	0.000000	−0.888670
$\Theta_{e\,A}$	Constant		121.07576			
k_B	P(+)	R_{OH-NN}	1.264759	2.549750	0.000000	−0.479980
$\Theta_{e\,B}$	Constant		114.46478			

HON

Parameter	Type	X	A	B	C	R_0
k	P(−)	R_{OH-NN}	1.164030	2.676090	0.000000	−1.002470
Θ_e	Constant		107.89000			

Table 1. Potential Energy Functions and Parameters (continued)

$V^{i}_{HONO} = \sum_{j=0}^{5} a_j Cos(j\tau)$

Parameter	Type	X	A	B	C	R_0
a_0	Constant		0.210699			
a_1	Constant		0.024922			
a_2	Constant		–0.192175			
a_3	Constant		–0.011035			
a_4	Constant		–0.005143			
a_5	Constant		–0.000555			

$V(\tau) = k[1 - Cos^2(\tau)]$

Parameter	Type	X	A	B	C	R_0
k(CNNO)	Constant		0.067100			
k(HCNN)	Constant		0.980000			

$V(\omega) = kCos^2(\omega)$

Parameter	Type	X	A	B	C	R_0
$k(NNO_2)$	Constant		1.260581			
$k(H_2CN)$	Constant		0.535061			

Attenuation Factors

Parameter	Type	X	A	B	C	R_0
$S_{NO(1)}$	P(–)	$R_{NO(1)}$	0.500000	5.000000	0.000000	3.500000
$S_{NO(2)}$	P(–)	$R_{NO(2)}$	0.500000	5.000000	0.000000	3.500000
S_{TT}	P(–)	R_{NN}	0.500000	20.00000	0.000000	2.500000
S_{Pro}	P(+)	R_{OH-NN}	0.500000	20.00000	0.000000	–1.370360
S_{OH-NN}	P(+)	R_{OH}	25.00000	6.000000	0.000000	2.350000

correctly describe this interaction at all regions of the PES. Also, some interactions do not exist at all regions of the PES and should be attenuated. Examples of these are the CNNO and HCNN torsional motions, as well as the CNN and NNO bends and NNO_2 out-of-plane wag. We have incorporated the required flexibility into equation (1) by using switching functions either to attenuate terms or to vary parameter values appropriately at the different regions of the PES. The forms of most of the switching functions and the parameters are either

$$P(+) = A\{1 + \tanh(B[X - R_0])\} + C \tag{2}$$

or

$$P(-) = A\{1 - \tanh(B[X - R_0])\} + C\ , \tag{3}$$

where X denotes the appropriate independent geometric variable. P(+) and P(–) vary continuously in the range of (2A + C) to C. The values of A, B, and C, as well as the definition of the independent geometric variable for the switching functions and parameters, are given in Table 1.

One independent geometric variable used to vary several of the parameters in equation (1) is defined as:

$$R_{OH\text{–}NN} = R_{OH} - R_{NN} + S_{OH\text{–}NN}\ . \tag{4}$$

R_{NN} is the N–N bond distance, and R_{OH} reflects a weighted contribution from each of the four possible O–H pairs in the molecule. The pairs are denoted as r_i, i = 14–17 and correspond to O–H pairs O(1)–H(1), O(2)–H(1), O(1)–H(2), and O(2)–H(2), respectively. R_{OH} is defined as:

$$R_{OH} = \sum_{i=14}^{17} r_i S_i\ , \tag{5}$$

where

$$S_i = \prod_{\substack{j=14 \\ j \neq i}}^{17} \left\{ \frac{1}{2}\left[1 - \tanh\left(b\left[r_i - r_j\right]\right)\right] \right\}\ . \tag{6}$$

The switching function S_{OH-NN} was added to equation (4) to eliminate the $(R_{OH}-R_{NN})$ dependence at regions of the PES where both R_{OH} and R_{NN} are very large.

The description of R_{OH} ensures that unless two or more H–O distances are equal, the R_{OH} description is defined by the shortest H–O bond. If any O–H distances are equal, the contribution to R_{OH} is divided evenly among the equal H–O bonds. R_{OH} is also used as the independent variable in the Morse function for the H–O stretching interaction.

The term to describe HON bending motions consists of weighted contributions from all possible HON angles (denoted θ_i, i = 14–17, where the H–O bond in the HON angle corresponds to r_i as defined previously).

$$V_{HON}^{b} = \sum_{i=14}^{17} \left[k\left(\theta_i - \theta_e\right)^2 \bullet S_i^{HON} \right], \tag{7}$$

where

$$\begin{aligned} S_{14}^{HON} &= S_{14}\,(1 + 2S_{15}) \\ S_{15}^{HON} &= S_{15}\,(1 + 2S_{14}) \\ S_{16}^{HON} &= S_{16}\,(1 + 2S_{17}) \\ S_{17}^{HON} &= S_{17}\,(1 + 2S_{16})\,. \end{aligned} \tag{8}$$

The model PES allows hydrogen migration in HONO; features of the saddle point for this hydrogen migration are discussed in the following section. This form of the HON bending potential describes the contribution of the two possible HON bends in HONO, which have an equal contribution when HONO is in the saddle point configuration for the hydrogen migration reaction.

The attenuation function, S_{HONO}, defined as

$$S_{HONO} = S_{NO(1)}\,(S_{14} + S_{16}) + S_{NO(2)}\,(S_{15} + S_{17})\,, \tag{9}$$

attenuates terms upon the secondary decomposition of HONO. This function also modifies the H–O interaction to correspond to that of the diatomic upon HONO decomposition.

The functional form of the parameters for some of the stretching and bending interactions are a bit more complex (see Table 1) than just P(+) or P(–) as defined in equations (2) and (3), for the following reason: The five-centered transition state leading to formation of HONO + HCN involves formation of an H–O bond while breaking a C–H bond. Because the CH_2NNO_2 molecule has two oxygens and two hydrogens, there are four possible H–O pairs that could form the HO bond in HONO (as one of two C–H bonds is broken). The potential energy function must be unbiased and invariant to any of these bond formations and scissions; i.e., HONO + HCN must be formed in the same manner regardless of which H–O pair forms the bond. Additionally, the N–O interaction in HONO is dramatically different depending on whether the oxygen in the NO moiety is terminal, bound to hydrogen, or is a free diatomic. The function must be able to discriminate in an unbiased fashion among all possible bonding situations. The added complexity of these functions, as well as inclusion of the various switching functions, accommodate these situations. Any modifications of parameter functional forms are given in Table 1.

2.2 Features of the PES. The chosen parameters ensure that the model reproduces measured properties of the products and reaction endothermicities as shown in Figure 2. The classical barrier heights for (I) and (II) differ by only 2 kcal/mol, with (I) being lower in energy at 35.0 kcal/mol. Geometric parameters, harmonic vibrational frequencies, and relative energies of the reactant, the products and the transition state are given in Table 2, along with the experimentally measured or theoretically determined information. The relative energies cited in Mowrey et al. (1990) are not included in Table 2, because the cited values are estimated activation energies, and include corrections for various levels of theory, different basis sets, and zero-point energy effects. The only uncorrected ab initio energy value to which we rigidly adhered in fitting the PES was the MRCI(DZ) energy difference between CH_2NNO_2 and HONO + HCN (–27.9 kcal/mol) in order to establish the relative energy position of the reactant.

The only information available about the reactant and saddle point leading to formation of HONO + HCN are the ab initio data of Mowrey et al. (1990; unpublished), which includes structures and matrices of energy second derivatives for the two stationary points, as well as several structures and energies along the reaction path leading from this saddle point. The most complete set of information provided by Mowrey et al. (1990; unpublished) are CASSCF/DZ structures and second derivatives which we have used for fitting the PES. The structural parameters of the PES at equilibrium are in exact

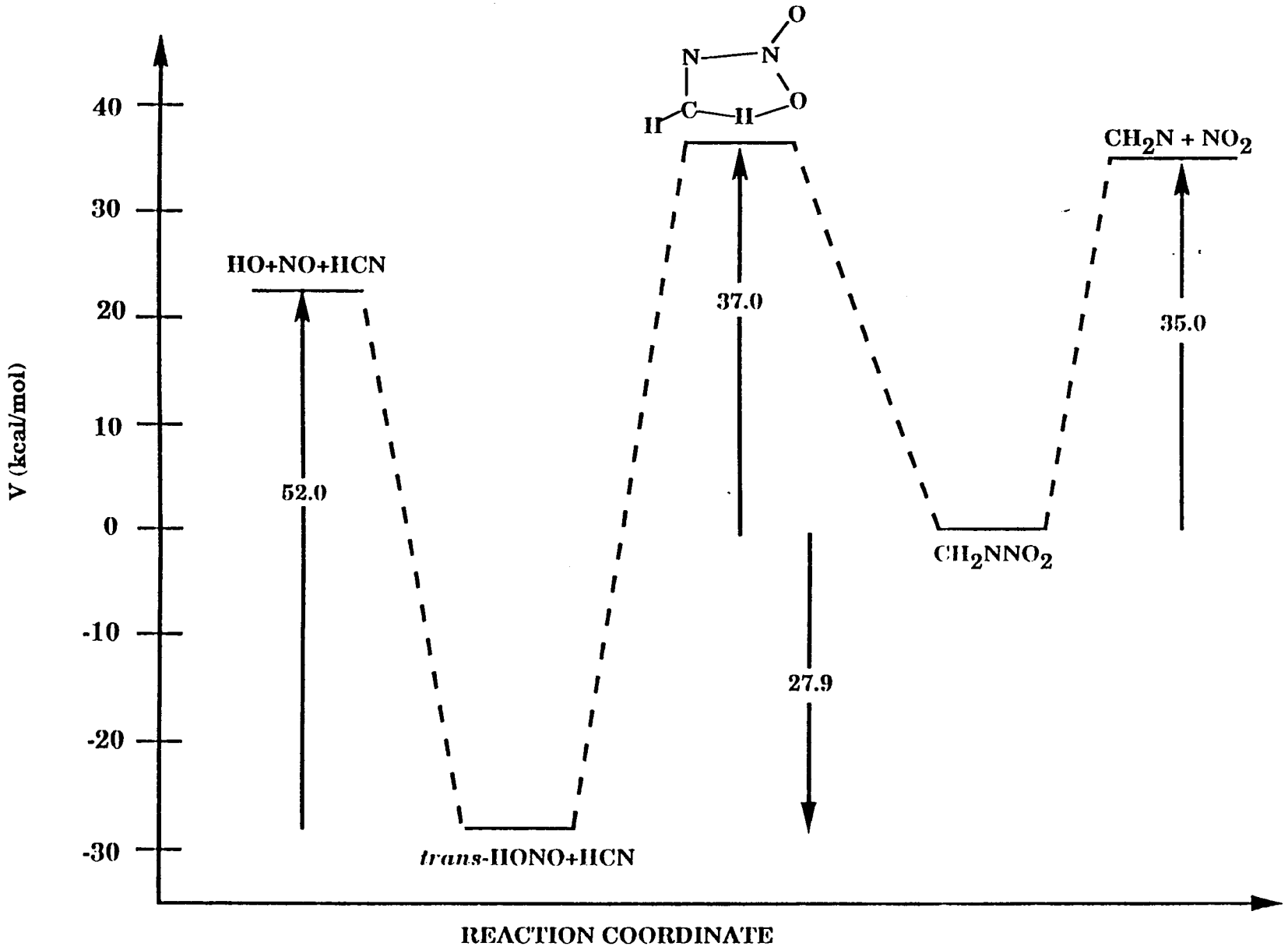

Figure 2. Energy level diagram for the CH_2NNO_2 PES (equation [1]), showing minima, saddle point energies, and asymptotic values of primary and secondary decomposition products.

Table 2. Structural Parameters, Zero Point Energies, and Relative Energies[a]

Internal Coordinate	CH_2NNO_2		Transition State		HONO + HCN			HO + NO + HCN			$H_2CN + NO_2$		
	Model	Ab initio	Model	Ab initio	Model	Expt.[b,c,d]	Ab initio	Model	Expt.[b,c,d]	Ab initio	Model	Expt.[b,c,d]	Ab initio
C_1N_1	1.271	1.271	1.216	1.216	1.150	1.157	1.151	1.149	1.157	1.151	1.271		1.263
N_1N_2	1.441	1.441	2.112	2.122	—	—	—	—	—	—	—		—
N_2O_2	1.240	1.240	1.226	1.226	1.400	1.432	1.484	—	—	—	1.244	1.197	1.199
N_2O_1	1.303	1.303	1.352	1.356	1.166	1.170	1.212	1.166	1.151	—	1.303	1.197	1.199
O_2H_1	—	—	1.399	1.407	0.954	0.958	0.988	0.954	0.971	—	—		—
C_1H_1	1.073	1.073	1.238	1.243	—	—	—	—	—	—	1.073		1.078
C_1H_2	1.071	1.071	1.070	1.071	1.065	1.058	1.054	1.065	1.058	1.054	1.071		1.078
$C_1N_1N_2$	115.7	115.7	91.4	91.6	—	—	—	—	—	—	—		—
$N_1N_2O_1$	114.5	114.5	134.1	134.1	—	—	—	—	—	—	—		—
$N_1N_2O_2$	121.1	121.1	105.3	105.1	—	—	—	—	—	—	—		—
$H_1C_1N_1$	124.1	124.1	110.4	110.2	—	—	—	—	—	—	124.1		120.9
$H_2C_1N_1$	116.0	116.0	129.2	129.2	180.0	180.0	180.0	180.0	180.0	180.0	116.0		120.9
$H_1O_2N_2$	—	—	90.2	90.1	107.9	102.1	103.5	—	—	—	—		—
$O_1N_2O_2$	124.4	124.4	120.6	120.8	111.4	110.7	109.3	—	—	—	124.4	134	137.1
Harmonic Frequencies	101	100	1287i	1257i	711	712	884	711	712	884	547	756.8	740
	275	391	208	231	711	712	884	711	712	884	1170	1357.8	1435
	560	561	165	335	2088	2089	2327	2088	2089	2327	1529	1665.5	1611
	442	621	514	342	3311	3312	3696	3311	3312	3696			
	606	665	319	495							1237		1094
	753	872	543	652	537	544	510	1778	1904		826		1167
	894	896	616	786	523	596	607				1434		1537
	1246	1220	919	789	841	790	816	3735	3735		1825		1817
	1268	1261	801	977	1261	1263	1306				3363		3292
	1323	1311	1074	1108	1703	1700	1619				3488		3397
	1454	1580	1297	1272	3592	3591	3611						
	1613	1612	1587	1622									
	1843	1839	1197	1873									
	3363	3361	2158	1911									
	3489	3482	3275	3442									
Zero Point Energy	27.5	28.3	21.0	22.6	21.8	21.9	23.2	17.6	17.8		22.0		23.0
Relative Energy	0.0	0.0	37.0		−27.9		−27.9	52.0	52.0		35.0		

[a] Distances given in Å, angles given in degrees, and energies given in kcal/mol.
[b] Herzberg (1945).
[c] Chase et al. (1985).
[d] Huber and Herzberg (1979).

agreement with the ab initio values. The transition state structure predicted by the model PES is in extremely close agreement with the ab initio structure, with the largest disagreement in a structural parameter being less than 0.5%. The structural parameters predicted by the model PES for the products ($H_2CN + NO_2$) and (HO + NO + HCN) are in fair agreement with the experimental and ab initio values; however, no effort was made to incorporate into the model PES the small structural changes as these products are formed. Differences in geometries between our model PES and the experimental and ab initio information for HONO + HCN are due to the use in the model PES of previously developed potential energy functions for HONO (Guan and Thompson 1989) and HCN (Waite 1984), with modifications to accommodate the thermochemistry of the system.

We have assigned the vibrational modes according to the eigenvectors rather than the values of the frequencies. Eigenvectors of the reactant, transition state, and products are in good agreement with the ab initio values (Mowrey et al. 1990) that are available, and can all be assigned. Agreement of the frequencies for some of the modes are poor. However, the results of our previous study (Rice et al. 1991) showed that good agreement of frequencies at the expense of the eigenvectors can drastically affect the reaction dynamics. Thus, we have used the ab initio eigenvectors for equilibrium MN and the five-centered transition state as the main fitting criteria for parameterizing the PES. Figure 3 shows the ab initio (Mowrey et al. 1990; unpublished) eigenvectors (3a) and eigenvectors obtained from our PES (3b) that correspond to the imaginary frequency of the transition state. The agreement is very good. Predicted frequencies of products by our model PES are in good agreement with the experimental values except for NO and NO_2, which result from the neglect of the modifications in the PES due to the slight changes in geometry and force constants as these products are formed.

Mowrey et al. (1990) estimate that the activation energy and A-factor for Reaction (II) are 31 ± 4 kcal/mol and 10^{13} s^{-1}, respectively. We refined the model PES using this information by calculating thermal rate coefficients for 200–1,500 K, and extracting Arrhenius parameters using canonical variational transition state theory (Truhlar, Isaacson, and Garrett 1985) and the POLYRATE 5.0.1 set of computer codes (Lu et al. 1992; Liu et al. 1993). Adjustments were made to the classical barrier height until the calculated activation energy was in agreement with the Mowrey et al. (1990) estimate.

Generalized transition state theory (GTST) rate constants (Truhlar, Isaacson, and Garrett 1985) have the form

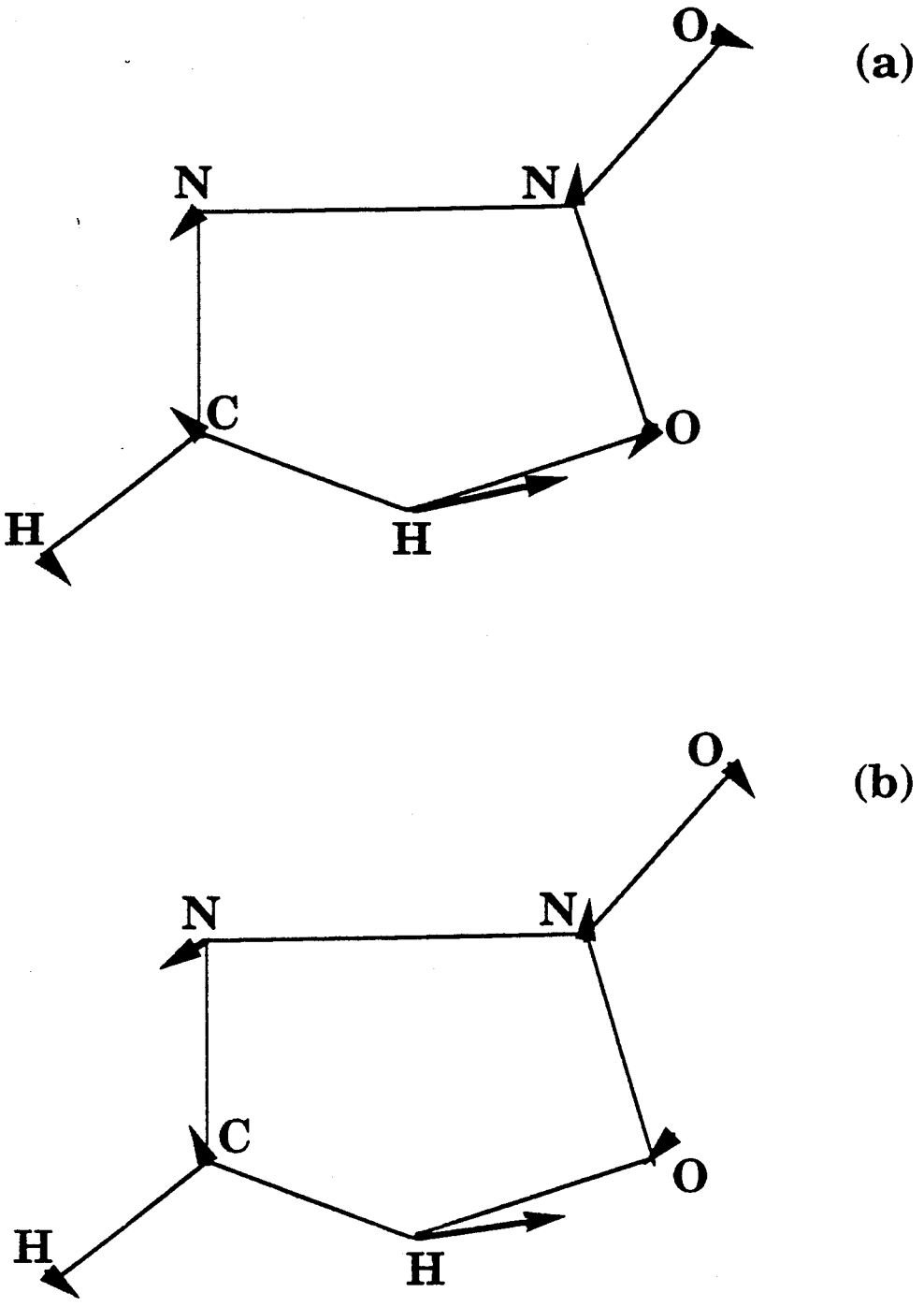

Figure 3. Depiction of the normal mode associated with the imaginary frequency of the transition state leading to HONO + HCN for a) ab initio prediction (see Mowrey et al. 1990) and b) that predicted by the model PES, equation (1).

$$k^{GT}(T,s) = \sigma \frac{K_b T}{h} \frac{Q^{GT}(T,s)}{Q^R(T)} \exp(-V_{MEP}(s) / k_b T), \quad (10)$$

where σ is a symmetry factor, T is the temperature, k_B and h are Boltzmann's and Planck's constants, respectively, and s is the distance along the reaction path from the saddle point. The reaction path is generally taken to be the minimum energy path (MEP) from the saddle point to the reactant and product geometries. $Q^{GT}(T,S)$ is the partition function for the bound degrees of freedom at the generalized transition state location, s, $Q^R(T)$ is the partition function of the reactant species, and $V_{MEP}(s)$ is the value of the potential energy at the generalized transition state location s. In canonical variational theory, the rate, $k^{CVT}(T)$, is obtained by optimizing equation (10) with respect to s. The conventional transition state theory rate, k‡(T), corresponds to s = 0.

We wish to point out that the rates calculated using equation (10) are not classical GTST rate constants, because the partition functions for the bound modes of the generalized transition states and the reactant are evaluated quantum mechanically. The reaction coordinate motion, however, is treated classically. Quantal effects on reaction coordinate motion are included by using multiplicative semiclassical ground-state adiabatic transmission coefficients

$$k^{CVT/Y}(T) = \kappa^Y k^{CVT}(T) \quad (11)$$

where Y is merely a label that denotes the various methods used to calculate these semiclassical transmission coefficients (Truhlar, Isaacson, and Garrett 1985). These coefficients generally account for quantum mechanical tunneling. Because Mowrey et al. (1990) did not include tunneling effects in their estimate of the activation energy, we used the VTST rates that treated reaction coordinate motion classically ($k^{CVT}[T]$) to refine the PES. The interested reader is referred to Truhlar, Isaacson, and Garrett (1985) for a detailed description of the theory, methods, approximations, and additional references.

Conventional and variational transition state theory rates for Reaction (II) are shown in Table 3. Arrhenius parameters shown in Table 3 were fitted over the temperature range 300–1,500 K. The $k^{CVT}(T)$ activation energy and A-factor are 31.8 kcal/mol and 4×10^{13} s^{-1}, respectively, in good agreement with the values estimated by Mowrey et al. (1990). The rates that include tunneling effects indicate that tunneling is not important at temperatures greater than 300 K, but is significant at lower temperatures.

Table 3. Thermal Rate Coefficients (s^{-1}) for $CH_2NNO_2 \rightarrow HONO + HCN$

T, K	‡	‡/CAG	‡/MEPSAG	‡/CD-SCSAG	CVT	CVT/CAG	CVT/MEPSAG	CVT/CD-SCSAG
200.00	2.33(–21)	1.71(–21)	1.49(–20)	8.25(–17)	1.67(–21)	1.67(–21)	1.45(–20)	8.04(–17)
300.00	4.86(–10)	3.96(–10)	7.56(–10)	1.83(–09)	3.73(–10)	3.72(–10)	7.09(–10)	1.71(–09)
500.00	7.66(–01)	6.77(–01)	8.28(–01)	1.07(–00)	5.80(–01)	5.60(–01)	6.84(–01)	8.87(–01)
1000.00	9.89(+06)	9.30(+06)	9.76(+06)	1.04(+07)	5.78(+06)	5.27(+06)	5.53(+06)	5.87(+06)
1500.00	2.84(+09)	2.72(+09)	2.78(+09)	2.86(+09)	1.35(+09)	1.18(+09)	1.21(+09)	1.24(+09)
E_a (kcal/mol)	32.2	32.3	31.9	31.2	31.8	31.7	31.3	30.6
log(A)	14.1	14.0	14.0	13.9	13.7	13.7	13.6	13.5

The reaction path energies reported by Mowrey et al. (unpublished) were given relative to the energy at the saddle point for (II). Therefore, the reaction path energies were shifted accordingly as adjustments in the height of the saddle point were made during refinement of the PES using VTST (Truhlar, Isaacson, and Garrett 1985). Figure 4 shows the results of the fit of the model PES (equation [1]) to the ab initio information. The circles denote the points along the ab initio reaction path (Mowrey et al. unpublished), the crosses denote the model PES (equation [1]) for the same structures, and the solid line is the reaction path (not including zero point energy) of the PES predicted by POLYRATE 5.0.1 (Lu et al. 1992; Liu et al. 1993). The reaction path predicted by our model is in good agreement on the reactant side of the saddle point (positive s). The agreement with ab initio on the product side (negative s) is not as good as for the reactant portion of the path, but is still reasonable. The discrepancies between the ab initio and the model PES energy curves are due to differences in predicted product geometries. To illustrate this, the N–N (circles), C–H (diamonds), and H–O (squares) bond distances along the reaction path are shown in Figure 5. The lines in this figure correspond to geometries along the model PES reaction path, and the symbols correspond to the ab initio values (Mowrey et al. unpublished). The model N–N and C–H bond distances are in very good agreement with the ab initio values all along the path, but the H–O distance toward the products differs by approximately 0.03 Å. This, and other slight differences in product geometries between the model PES and ab initio calculations explain the energy differences for large negative s values.

Figure 6 shows the potential energy as a function of the N–N distance. For each fixed value of the N–N distance shown in this figure, the remaining internal coordinates have been relaxed to the geometry at which the first derivative of the energy with respect to all remaining coordinates is zero. As expected, this results in an energy profile path for Reaction (I) that has no barrier beyond its endothermicity.

We also found a saddle point leading to hydrogen-atom migration in HONO. The structure of the transition state species is almost square; the HON angles are 91.2°, the ONO angle is 91.0°, and the N–O and H–O bonds are 1.2340 and 1.1313 Å, respectively. The barrier to hydrogen migration in HONO predicted by this model (51.4 kcal/mol) is slightly less than the dissociation to HO + NO (52.0 kcal/mol). The actual migration barrier is likely considerably lower than our model PES predicts. We do not expect this higher migration barrier to affect the results and conclusions of our planned dynamics study, which will focus mainly on the primary decomposition reactions of CH_2NNO_2.

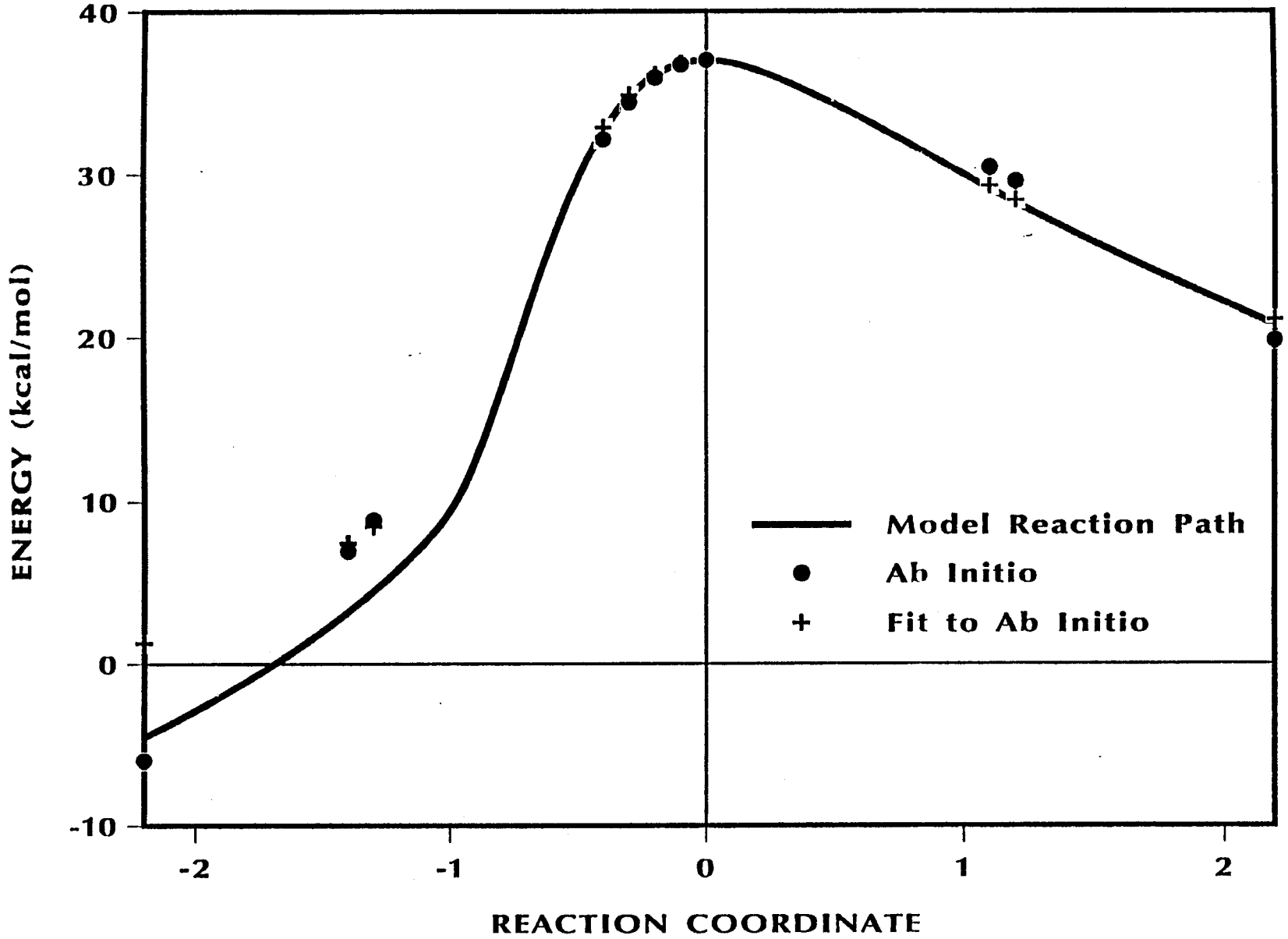

Figure 4. Potential energy of the reaction path leading to HONO + HCN. Filled circles denote ab initio predictions (Mowrey et al. unpublished), crosses are the energies predicted by equation (1) using the ab initio geometries, and the solid line is the reaction path predicted by equation (1), using POLYRATE 5.0.1 (Lu et al. 1992; Liu et al. 1993).

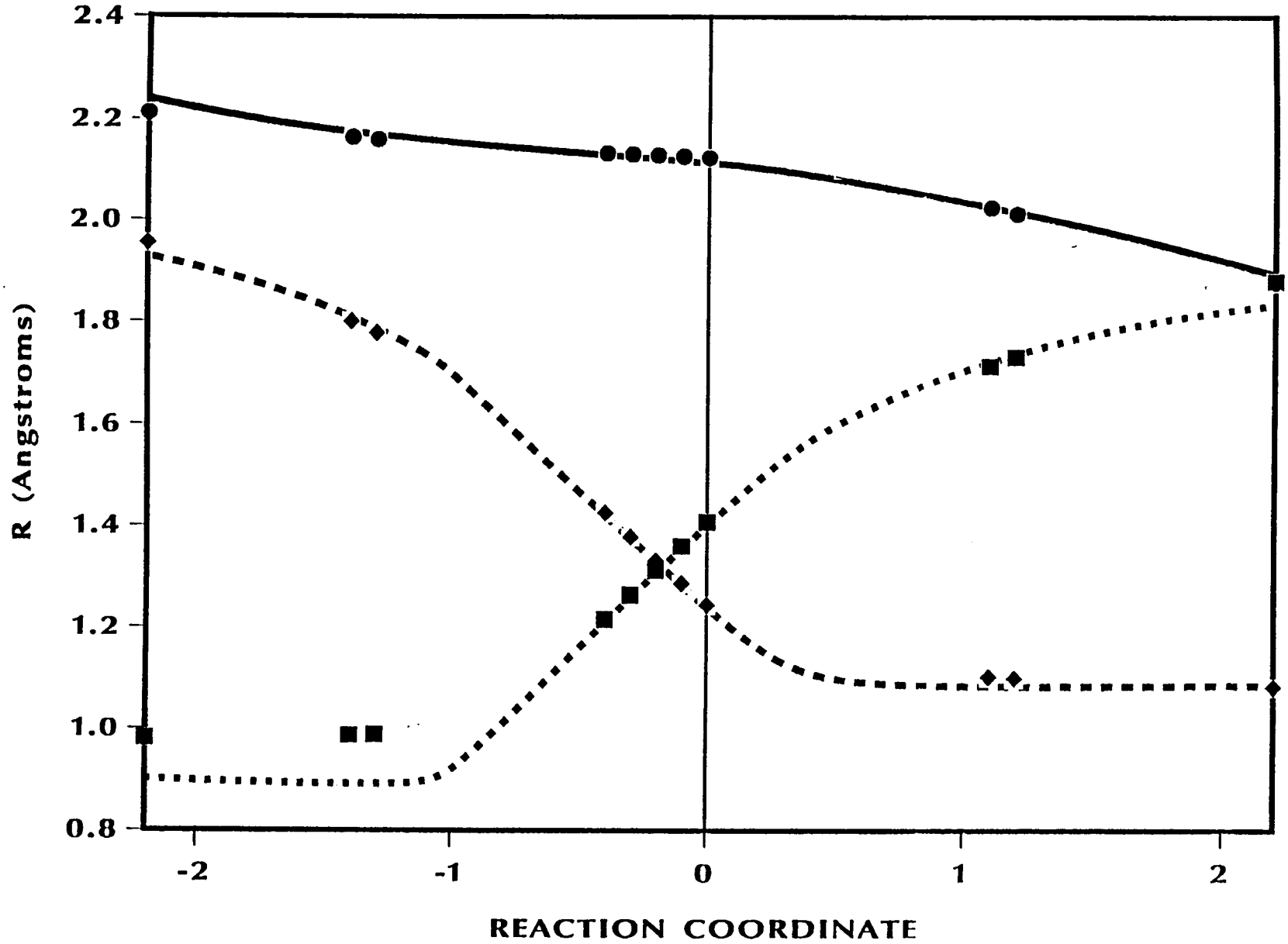

Figure 5. N–N (circles), C–H (diamonds), and H–O (squares) internuclear distances at points along the reaction path shown in Figure 4. The points are the ab initio values (Mowrey et al. unpublished), and the lines are the corresponding internuclear distances along the reaction path predicted by equation (1). The model N–N distances are denoted by a solid line, the C–H distances are denoted by a long-dashed line, and the H–O distances are denoted by a short-dashed line.

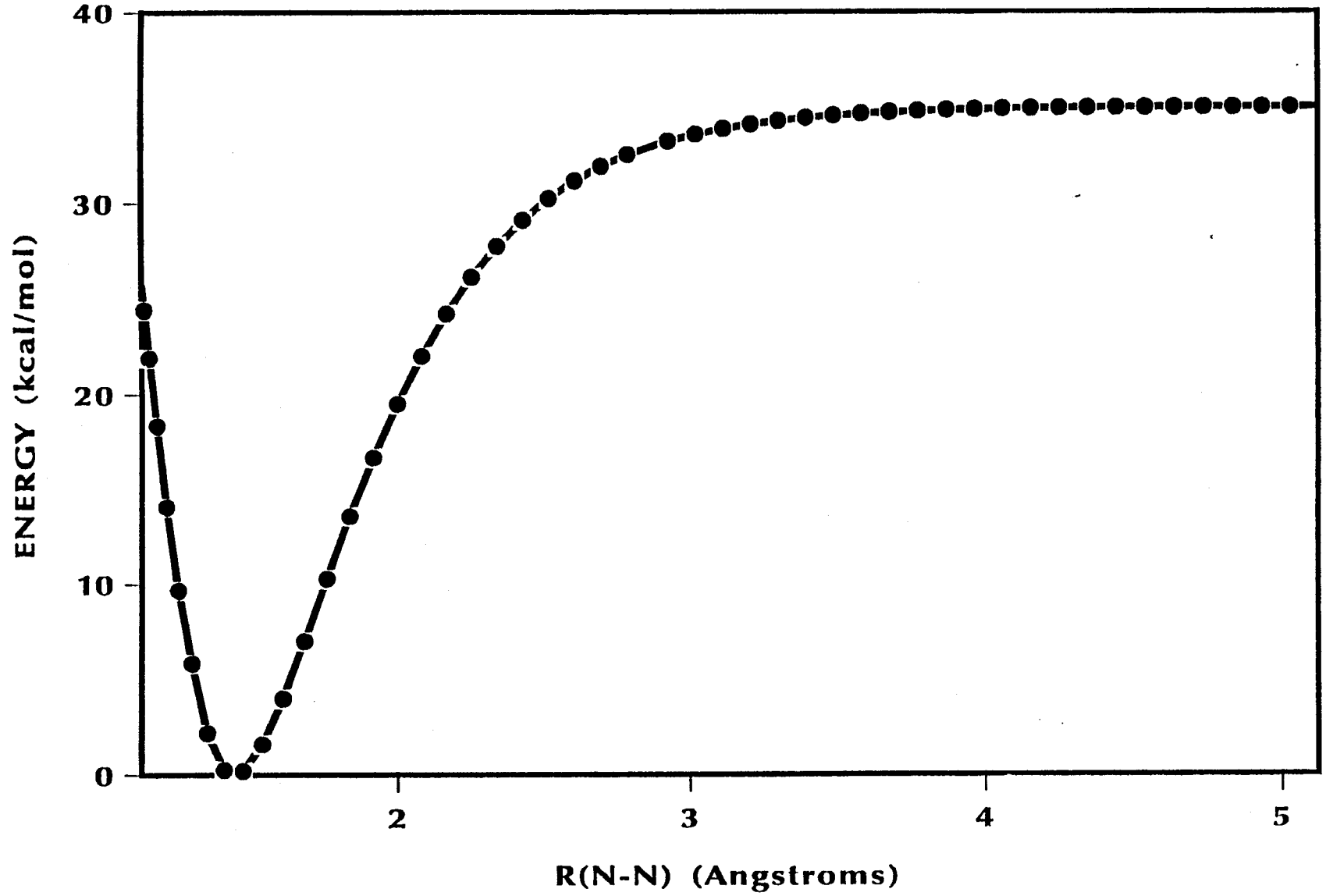

Figure 6. Potential energy as a function of N–N distance predicted by equation (1). All internal coordinates of the MN molecule are relaxed to the equilibrium position (gradients are zero) for each N–N distance in this figure.

3. SUMMARY

We have developed and reported the analytic PES for MN, which can be used in molecular dynamics simulations of the unimolecular decomposition of CH_2NNO_2. The potential energy function incorporates ab initio MCSCF and MRCI calculations (Mowrey et al. 1990; unpublished) of critical points for two competing reaction paths:

$$CH_2NNO_2 \rightarrow H_2CN + NO_2 \qquad (I)$$

and

$$CH_2NNO_2 \rightarrow HCN + HONO\ . \qquad (II)$$

The bond dissociation energy for N–N bond scission in (I) is 35 kcal/mol; this reaction has no back reaction barrier. The activation energy of (II) has been estimated to be 31 ± 4 kcal/mol based on the ab initio calculations (and corrections) by Mowrey et al. (1990). The transition state for this reaction is a five-centered cyclic structure with a classical barrier of 37 kcal/mol. The barrier height corresponding to this transition state was adjusted to predict a thermal activation energy of 31.8 kcal/mol, in agreement with the Mowrey et al. (1990) estimates. Additionally, matrices of the energy second derivatives for stationary points and points along the reaction paths that were calculated by Mowrey et al. (unpublished) were used in parameterizing the PES.

Thermal rates for (II) were calculated using Variational Transition State Theory (Truhlar, Isaacson, and Garrett 1985) and used to adjust the PES until they were in agreement with the Mowrey et al. estimates (Mowrey et al. 1990). Tunneling effects in (II) are significant only at low temperatures, and do not contribute appreciably to the rate of decomposition at the energies considered in this study.

4. REFERENCES

Chase, M. W., C. A. Davies, J. R. Downey, D. J. Frurip, R. A. McDonald, and A. N. Syverud. JANAF Thermochemical Tables, 3rd Ed., Journal of Physical Chemistry, Ref. Data 14, Supplement 1, 1985.

Guan, Y., and D. L. Thompson. Chemical Physics, vol. 139, p. 147, 1989.

Herzberg, G. Infrared and Raman Spectra of Polyatomic Molecules. Princeton: Van Nostrand, 1945.

Huber, K. P., and G. Herzberg, Constants of Diatomic Molecules. New York: Van Nostrand Reinhold, 1979.

Liu, Y. -P., G. C. Lynch, W. -P. Hu, V. S. Melissas, R. Steckler, B. C. Garrett, D. -h. Lu, T. N. Truong, A. D. Isaacson, S. N. Rai, G. C. Hancock, J. G. Lauderdale, T. Joseph, and D. G.Truhlar. POLYRATE, QCPE Program 601-version 5.0.1; Quantum Chemistry Program Exchange, Indiana University, Bloomington, IN, 1993; QCPE Bulletin, vol. 13, pp. 28–29 (1993).

Lu, D. -h., T. N. Truong, V. S. Melissas, G. C. Lynch, Y. -P. Liu, B. C. Garrett, R. Steckler, A. D. Isaacson, S. N. Rai, G. C. Hancock, J. G. Lauderdale, T. Joseph, and D. G. Truhlar. Computer Physics Communications, vol. 71, p. 235, 1992.

Mowrey, R. C., M. Page, G. F. Adams, and B. H. Lengsfield, III. Unpublished.

Mowrey, R. C., M. Page, G. F. Adams, and B. H. Lengsfield, III. Journal of Chemical Physics, vol. 93, p. 1857, 1990.

Rice, B. M., C. F. Chabalowski, G. F. Adams, R. C. Mowrey, and M. Page. Chemical Physics Letters, vol. 184, p. 335, 1991.

Schroeder, M. A. "Critical Analysis of Nitramine Decomposition Data: Product Distributions From HMX and RDX Decomposition." BRL-TR-2659, U.S. Army Ballistic Research Laboratory, Aberdeen Proving Ground, MD, June 1985a.

Schroeder, M. A. "Critical Analysis of Nitramine Decomposition Data: Activation Energies and Frequency Factors for HMX and RDX Decomposition." BRL-TR-2673, U.S. Army Ballistic Research Laboratory, Aberdeen Proving Ground, MD, September 1985b.

Truhlar, D. G., A. D. Isaacson, and B. C. Garrett. Theory of Chemical Reaction Dynamics. Edited by M. Baer, vol. 4, Boca Raton, FL: CRC Press, 1985.

Waite, B. A. Journal of Physical Chemistry, vol. 88, p. 5076, 1984.

Zhao, X., E. J. Hinsta, and Y. T. Lee. Journal of Chemical Physics, vol. 88, p. 801, 1988.

INTENTIONALLY LEFT BLANK.

NO. OF COPIES	ORGANIZATION
2	ADMINISTRATOR ATTN DTIC DDA DEFENSE TECHNICAL INFO CTR CAMERON STATION ALEXANDRIA VA 22304-6145
1	COMMANDER ATTN AMCAM US ARMY MATERIEL COMMAND 5001 EISENHOWER AVE ALEXANDRIA VA 22333-0001
1	DIRECTOR ATTN AMSRL OP SD TA US ARMY RESEARCH LAB 2800 POWDER MILL RD ADELPHI MD 20783-1145
3	DIRECTOR ATTN AMSRL OP SD TL US ARMY RESEARCH LAB 2800 POWDER MILL RD ADELPHI MD 20783-1145
1	DIRECTOR ATTN AMSRL OP SD TP US ARMY RESEARCH LAB 2800 POWDER MILL RD ADELPHI MD 20783-1145
2	COMMANDER ATTN SMCAR TDC US ARMY ARDEC PCTNY ARSNL NJ 07806-5000
1	DIRECTOR ATTN SMCAR CCB TL BENET LABORATORIES ARSENAL STREET WATERVLIET NY 12189-4050
1	DIR USA ADVANCED SYSTEMS ATTN AMSAT R NR MS 219 1 R&A OFC AMES RESEARCH CENTER MOFFETT FLD CA 94035-1000

NO. OF COPIES	ORGANIZATION
1	COMMANDER ATTN AMSMI RD CS R DOC US ARMY MISSILE COMMAND REDSTONE ARSNL AL 35898-5010
1	COMMANDER ATTN AMSTA JSK ARMOR ENG BR US ARMY TANK AUTOMOTIVE CMD WARREN MI 48397-5000
1	DIRECTOR ATTN ATRC WSR USA TRADOC ANALYSIS CMD WSMR NM 88002-5502
1	COMMANDANT ATTN ATSH CD SECURITY MGR US ARMY INFANTRY SCHOOL FT BENNING GA 31905-5660
	ABERDEEN PROVING GROUND
2	DIR USAMSAA ATTN AMXSY D AMXSY MP H COHEN
1	CDR USATECOM ATTN AMSTE TC
1	DIR USAERDEC ATTN SCBRD RT
1	CDR USACBDCOM ATTN AMSCB CII
1	DIR USARL ATTN AMSRL SL I
5	DIR USARL ATTN AMSRL OP AP L

INTENTIONALLY LEFT BLANK.

USER EVALUATION SHEET/CHANGE OF ADDRESS

This Laboratory undertakes a continuing effort to improve the quality of the reports it publishes. Your comments/answers to the items/questions below will aid us in our efforts.

1. ARL Report Number ARL-TR-680 Date of Report February 1995

2. Date Report Received _____

3. Does this report satisfy a need? (Comment on purpose, related project, or other area of interest for which the report will be used.) _____

4. Specifically, how is the report being used? (Information source, design data, procedure, source of ideas, etc.) _____

5. Has the information in this report led to any quantitative savings as far as man-hours or dollars saved, operating costs avoided, or efficiencies achieved, etc? If so, please elaborate. _____

6. General Comments. What do you think should be changed to improve future reports? (Indicate changes to organization, technical content, format, etc.) _____

CURRENT ADDRESS

_____
Organization

_____
Name

_____
Street or P.O. Box No.

_____
City, State, Zip Code

7. If indicating a Change of Address or Address Correction, please provide the Current or Correct address above and the Old or Incorrect address below.

OLD ADDRESS

_____
Organization

_____
Name

_____
Street or P.O. Box No.

_____
City, State, Zip Code

(Remove this sheet, fold as indicated, tape closed, and mail.)
(DO NOT STAPLE)

DEPARTMENT OF THE ARMY

OFFICIAL BUSINESS

NO POSTAGE
NECESSARY
IF MAILED
IN THE
UNITED STATES

BUSINESS REPLY MAIL
FIRST CLASS PERMIT NO 0001, APG, MD

Postage will be paid by addressee

Director
U.S. Army Research Laboratory
ATTN: AMSRL-OP-AP-L
Aberdeen Proving Ground, MD 21005-5066